Future Energy Open Access Journal

ISSN 2832-0328

Journal homepage: https://fupubco.com/fuen



https://doi.org/10.55670/fpll.fuen.4.4.4

Article

Optimizing heliostat solar power plant field design: using the golden ratio of the Fibonacci sequence

Seyed Farhan Moosavian, Ahmad Hajinezhad*

Engineering and Sustainable Resources, College of Interdisciplinary Science and Technologies, University of Tehran, Iran

ARTICLE INFO

Article history:
Received 22 July 2025
Received in revised form
29 August 2025
Accepted 12 September 2025

Keywords: Heliostat solar power plant, Fibonacci Golden Ratio, Optical efficiency coefficients, Radial field, Solar thermal system

*Corresponding author Email address: hajinezhad@ut.ac.ir

DOI: 10.55670/fpll.fuen.4.4.4

ABSTRACT

Considering the importance of achieving sustainable development and using the potential of clean and renewable energy resources, such as solar energy with the highest efficiency, this research aims to optimize the design of the Heliostat solar power plant field with a central tower using the golden ratio of the Fibonacci sequence and investigate the effect of this ratio on the designed field results. The reference pattern used in this paper is the radial staggered pattern. The field under study is located in Naypyitaw (the capital of Myanmar). In this paper, with the approach of optimizing the heliostat field design, using the equations available in the design of solar power plants, the results of the new field pattern calculated using the golden ratio are investigated. The results of this research show that using the golden ratio increases the area required for the placement of heliostats by 27%, while increasing the optical efficiency by 77%. Also, in this case, it will be possible to increase the number of heliostats by 11% without increasing the current area.

1. Introduction

Today, with the development of cities and the increase in population, per capita energy consumption is increasing rapidly [1]. Also, with the increase in developing countries, the intensity of energy consumption and fossil fuels has been increasing [2]. Since fossil fuels are a finite and nonrenewable resource, humanity is forced to find ways to replace these types of energy sources with renewable sources with less pollution to the environment [3]. Currently, many environmental problems have arisen due to the use of fossil fuels, including damage to the ozone layer, air and water pollution, the loss of animal species, global warming, and rising sea levels [4]. The most important solution to preserve fossil energy resources and achieve sustainable development is to pay attention to renewable energy sources, including solar energy [5, 6]. The sun is a real and free source of energy [7]. The use of solar energy as a source of energy for largescale uses is one of the hopes of the future [8]. The major problems in the use of solar energy are its lack of concentration, periodicity, and inconsistency in the amount of radiation [9]. If a means can be made to concentrate it so that its fluctuations do not have much effect on it, a very large energy source has been achieved that can supply human energy needs for centuries [10]. Given the state of energy in the world and the growth of population and consumption, if we act wisely, we will see that the sun is the only energy source that is abundantly and freely available at all times.

Additionally, there are no environmental pollution issues related to converting solar energy [11,12]. This energy can be used in all regions of the world. Solar energy will be available as long as the sun exists. Solar energy can be obtained in various ways [13]. This energy can be converted into heat or electricity and used. One of the methods of obtaining solar energy is to use a thermal power plant with a central receiver [14, 15]. In these power plants, solar radiation is focused by a field of many reflecting mirrors called heliostats onto a receiver located at the top of a tall tower [16]. At the focus point, a lot of thermal energy is generated, which is absorbed by the working fluid moving inside the receiver. These power plants are designed in different ways. There are various layouts for heliostats, each with its own advantages and disadvantages [17]. Therefore, if a more optimal solution for the layout of heliostats in thermal power plants with a central receiver can be achieved, it is possible to obtain more energy output from these power plants by increasing productivity and efficiency, which is a significant advance in the heliostat power plant [18]. Given the importance of developing solar thermal power plants in recent years, extensive research has been conducted in the field of heliostat power plants. These studies have mainly focused on the areas of heliostat array layout methods and improving optical efficiency. In this regard, Noone et al. presented a new computationally efficient model and biomimetic layout design for heliostat fields. According to their model, in a field with 1000 heliostats, the

field area is reduced by 18.1% compared to the base field. This reduction reaches 18.7% in the case of 2000 heliostats and 18.5% in the case of 3000 heliostats [19]. In another study, Basarti et al. [20] presented an efficient computational method for heliostat field design. They used a genetic algorithm to optimize the biomimetic field. Compared with previous methods, they showed that this method is able to accurately predict the shading coefficient. Also, with the help of this method, the maximum annual radiation optical efficiency of 68.3% was obtained, while the number of heliostats decreased from 624 to 594. Mutuberria et al. [21] conducted a comparison of heliostat field design methods and their impact on plant efficiency. Their study focused on dense radial staggered, Campo arrays, Graphical arrays, DELSOL arrays, and Fermat spiral. Comparing these arrays, they concluded that the Fermat spiral had the highest efficiency of 74.2%, and dense radial staggered had the lowest efficiency of 68.9%. Richter et al. [22] presented an evolutionary algorithm for designing an optimal heliostat field and compared it with the PS10 field and the biomimetic field. The new design achieved an efficiency of 68.71%, compared to 66.51% for the PS10 field and 67.51% for the biomimetic field.

Deng et al. [23] presented the Rose pattern for radial fields. Radial fields are considered suboptimal fields. The radial field efficiency increased from 44.38% in the suboptimal case to 53.97% using the Rose pattern. Xie et al. [24] studied the improved Gray Wolf pattern method to optimize the heliostat field. According to the results of their study, the heliostat field efficiency increased by 8.7%. Also, the number of heliostats was reduced from 8928 to 2509 compared to the base field. Another group of researchers has focused on optimizing the spacing of heliostat arrays with the aim of increasing the optical efficiency. In this regard, Ghirardi et al. presented an optimization process to investigate the possibility of determining the radial spacing of heliostat rows, the tower height, and the location of each individual heliostat. The resulting layouts show maximum field efficiency between 64.78% and 65.77% [25]. In another study, Kashif Ali et al. [26] proposed a new heliostat field layout method based on the Campo design method coupled with an adaptive gravity search algorithm (AGSA). The heliostat field in the layout process is 1.5 times larger than the final heliostat field. After setting the relevant constraints, the AGSA is used to find the best combination of spacing for maximizing energy efficiency of the heliostat field. Finally, according to the design requirements, the inefficient heliostats are eliminated to obtain the final layout of the heliostat field. As mentioned, various studies have been conducted in the field of heliostat layouts. These studies have focused on comparing different types of arrangements and evaluating their efficiency, improving and redesigning existing arrangements, and exploring new fields. One of these fields is the radial field, which, despite its extensive advantages, is one of the weakest fields in terms of efficiency and coefficient of performance. Regarding this type of field arrangement, new studies and patterns have been presented, such as the rose pattern, but again, its efficiency is lower than that of other arrangements. Hence, there is less acceptance in this field. One of the innovations in this field is the use of new patterns to redefine this type of arrangement. The pattern of the field arrangement is one of the main factors affecting the efficiency of the power plant, and the shading and blocking coefficients, the cosine coefficient, and also the total allowed number of Heliostats.

One of the recurring patterns in nature is the Fibonacci pattern [27]. This expression, which is simply an expression of the sum of two consecutive terms to obtain the next term, has been found in different parts of life, nature, and mathematical concepts. Examining this sequence led to the discovery of the golden ratio [28]. The golden ratio is obtained by dividing two consecutive numbers of this sequence and is equal to 1.618. The golden ratio is known by mathematicians as the ideal ratio. It is said that if this ratio is applied in any way, it will have an interesting result [27]. Therefore, as an interesting idea in this research, an attempt has been made to investigate and evaluate the concept of Fibonacci and the golden ratio, and the effect of this ratio on the efficiency of the Heliostat power plant. Previously, the concept of the Fibonacci sequence was used in the design of photovoltaics [29]. Still, the effects of the direct golden ratio in the design of the radial staggered field of the heliostat power plant have not been investigated so far. The purpose of this article is to achieve this and develop an innovative model for the design of heliostat fields. In this research, an attempt has been made to study the changes of the heliostat field by examining the design results of the pattern based on the golden ratio and comparing it with the basic pattern. Also, while examining the design results, the optical efficiency coefficients, field characteristics, and the improvements and limitations of the new field are explained.

2. Governing equations

The basic operation of thermal power plants is such that solar energy is first converted into thermal energy, and then, through a thermodynamic cycle such as the Brayton cycle. Rankine cycle, or combined cycle, thermal energy is converted into electrical energy [30, 31]. Generally, facilities that convert the thermal energy absorbed from the sun into electricity are called solar thermal power plants. Concentrated solar power plants have the potential to provide solar electrical energy at a lower cost than photovoltaic power plants. Concentrated solar power plants work by concentrating the incoming solar radiation into a small area using reflectors [32]. Concentrated solar systems operate in two ways: point concentration and linear concentration. Linear concentration systems are easier to implement, but they have a lower concentration ratio, which means they reach lower temperatures compared to point concentration systems. The different types of these power plants are illustrated in Figure 1 [33].

In power plants that operate with solar thermal systems to generate electricity, unlike photovoltaic systems, the presence of a heat transfer fluid to transfer the thermal energy absorbed by the receiver and a thermodynamic cycle to convert this heat into electricity is essential [34]. Central receiver solar power plants (CRS) are one of the most important types of solar power plants that have garnered attention due to their ability to reach high temperatures and suitable thermal efficiency. Additionally, it is possible to construct such a power plant on a much larger scale [35].

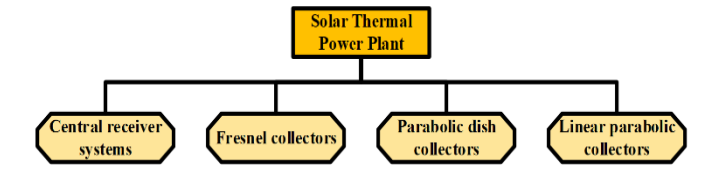


Figure 1. Types of solar thermal power plants



Figure 2. Heliostat solar power plant

In these power plants, as shown in Figure 2, solar radiation is concentrated onto a collector located at the top of a tall tower by reflecting mirrors called heliostats, which are arranged on tracks at specific distances from each other; thus, concentration in this type of system occurs at a point [36]. The central receiver systems exhibit a high concentration ratio, resulting in the generation of substantial thermal energy within the receiver. This energy is subsequently absorbed by the heat transfer fluid circulating within the receiver [37]. In instances where the heat transfer fluid coincides with the working fluid of the cycle, the fluid, upon absorbing thermal energy in the receiver, proceeds directly into the power generation cycle (direct case). Conversely, if the heat transfer fluid differs from the working fluid of the cycle, the energy acquired by the heat transfer fluid in the receiver is conveyed to the power generation cycle within the power plant via a heat exchanger (indirect case) [38]. CSP plants, which stand for Concentrated Solar Power, are going to be the future of electricity production in many countries around the world. These plants consist of a large number of individual solar tracker units, known as heliostats [39]. The goal of these heliostats is to focus the incoming rays onto a central tower. The performance of heliostat plants is measured by a ratio called optical efficiency, which is calculated by dividing the total power absorbed by the receiver by the total solar energy incident on the field. Most heliostat fields are designed in a radial configuration. This layout ensures that none of the heliostats in an adjacent ring block the reflected rays from hitting others. Since 50% of the total cost of heliostat plants and nearly 40% of the energy loss is related to the heliostat field, the design and layout of these fields are important [40]. To dynamically model a heliostat solar tower system (or a concentrated solar power plant), several key parameters and equations must be considered. These relationships include equations related to solar energy, the geometry of the heliostat system, the thermal behavior of the solar tower, and the system's efficiency over time. Below are the details of these equations.

2.1 Heliostat field design

In the design of radial fields, another heliostat is positioned in the adjacent rows between each pair of heliostats, which reduces the amount of shading caused by one heliostat on another. Figure 3 presents the basic definitions of the heliostat field, each of which will be examined in detail.

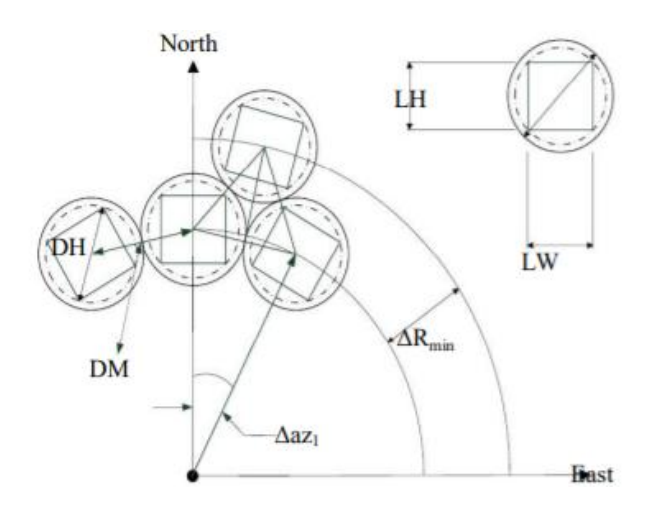


Figure 3. Heliostat field layout

The effective diameter is a characteristic that indicates the vertical distance between the centers of two adjacent heliostats, derived from Equation (1) [21].

$$DM = \sqrt{l_w^2 + l_h^2} + desp \tag{1}$$

In this equation, DM is the effective diameter, l_w is the length and l_h is the width of the heliostats, and desp indicates any extra distance between the heliostats. All variables are measured in meters.

The minimum radial distance of heliostats in adjacent rows to ensure they don't collide with each other is derived from Equation (2) [41].

$$\Delta R_{min} = DM \times \cos 30^{\circ} \tag{2}$$

The effect of the golden ratio of Fibonacci will be taken into account in this parameter, and in fact, the radial distance between the heliostats is defined by the golden ratio.

Additionally, the radial distance from the first row to the central tower is calculated using Equation (3) [41].

$$R_1 = Nhel_1 \times \frac{DM}{2\pi} \tag{3}$$

In Equation (3), $Nhel_1$ is the heliostat's number in each row of the first zone. The angular distance of the azimuth for the first zone of the field can be calculated using Equation (4) [41].

$$\Delta a z_1 = 2 \sin^{-1} \frac{DM}{2R_1} \tag{4}$$

 Δaz_1 that is the azimuth angular distance in the first zone measured in radians. The above equation can also be calculated for other zones. The azimuth angular distance for zone i is calculated using Equation (5) [41].

$$\Delta a z_i = \frac{\Delta a z_1}{2^{i-1}} \tag{5}$$

To calculate the radial distance of zone i from the central tower, Equation (6) is used [41].

$$R_i = 2^{i-1} \times \frac{DM}{\Delta a z_1} \tag{6}$$

Using the above equations, the radial distance and angular distance from the central tower can be determined for all zones.

To calculate the number of rows in zone i based on the radial distance of zone i, Equation (7) is used [42].

$$Nrow_i = \frac{R_{i+1} - R_i}{\Delta R_{min}} \tag{7}$$

The number of heliostats in each row is calculated from Equation (8) [42].

$$Nhel_i = \frac{2\pi}{\Delta a z_i} \tag{8}$$

2.2 Optical efficiency

Optical Efficiency measures the energy wasted in the heliostat field is obtained from Equation (9) [43].

$$\eta_{opt} = \eta_{at} \times \eta_{ref} \times \eta_{s\&b} \times \eta_{cos} \tag{9}$$

In this relation, η_{at} is the atmospheric attenuation coefficient, η_{ref} is the mirror reflection coefficient, $\eta_{s\&b}$ is the shading and blocking coefficient, and η_{cos} is the cosine coefficient. The mirror reflection coefficient can be considered a constant value, which is equal to 0.95. The remaining coefficients are calculated according to the heliostat field layout, receiver height, and other relevant parameters.

This coefficient expresses the effect of the reflected ray's energy that is absorbed or scattered by the atmosphere. This coefficient depends on the weather conditions and the distance of the heliostat from the receiver. This coefficient is obtained from relations (10), (11) [43].

 $if \ d \le 1000m,$

$$\eta_{at} = 0.99321 - 0.0001176d + 1.97 \times 10^{-8} \times d^2$$
 (10)

if d > 1000m,

$$\eta_{at} = e^{-0.0001106d} \tag{11}$$

In these two equations, d represents the distance between the heliostat and the receiver.

Shading occurs when the shadow of one heliostat falls on another. This coefficient depends on many factors, including time, and its calculation varies with time. The annual average value of this coefficient is 0.944.

The greatest energy loss in a heliostat field is related to the angle between the sun's rays and the normal vector to the heliostat surface. The smaller this angle, the lower the loss. The ideal value of this angle is when the radiation beam is perpendicular to the heliostat surface. This angle depends on both the sun and the tower design.

2.3 Solar position

The position of the sun is constantly changing throughout the day, and it is very important. The solar declination is calculated from Equation (12) [44].

$$\delta_s = 23.45 \sin(\frac{^{360}}{^{365}}(284 + N)) \tag{12}$$

In this equation, N is the number of days. The solar hour angle is also calculated from Equation (13) [45].

$$h_s = (Solar\ hour\ -12) \times 15^{\circ} \tag{13}$$

The solar altitude angle is calculated from Equation (14) [46].

$$\alpha_s = \sin^{-1}[\cosh(h_s).\cos(\delta_s).\cos(\phi_{lat}) + \sin(\delta_s).\sin(\phi_{lat})]$$
(14)

In the next step, the zenith angle is calculated using equation (15) [45].

$$\theta_z = 90^{\circ} - \alpha_s \tag{15}$$

To obtain the solar azimuth angle, it is necessary to calculate the solar azimuth factor, which is obtained from equation (16) [44].

$$\varphi' = \sin^{-1}(\frac{\cos \delta_s \times \sinh_s}{\sin \theta_s}) \tag{16}$$

Equations (17) and (18) are used to calculate the solar azimuth angle [44].

$$\varphi_s = 180^{\circ} - \varphi^{/} \text{ if } \cos h_s \ge (\frac{\tan \delta_s}{\tan \theta_{lat}})$$
 (17)

$$\varphi_s = 180^{\circ} + \varphi' \ if \ \cos h_s \le \left(\frac{\tan \delta_s}{\tan \phi_{lat}}\right)$$
 (18)

The azimuth angle of the surface is also calculated using Equations (19) and (20) [44].

if
$$\varphi_s - \varphi' > 0$$
, $\varphi_{surf} = \varphi' + 90^\circ$ (19)

Else
$$\varphi_s - \varphi' < 0$$
, $\varphi_{surf} = \varphi' - 90^{\circ}$ (20)

2.4 Receiver tower design

The design of the receiver tower is of great importance to absorb the maximum reflected rays. The reflected rays' angle with the receiver aperture (θ_R) and the angle between the reflected rays and the line perpendicular to the receiver surface (λ_s) are calculated using Equations (21) and (22) [47].

$$\theta_R = \sin^{-1}(\frac{-2dl + L\sqrt{4l^2 + L^2 - d^2}}{4l^2 + L^2}) \tag{21}$$

$$\lambda_{\rm s} = 90^{\circ} - \theta_{\rm R} \tag{22}$$

In the above equations, d is the diameter of the reflected area, l is the length of the reflector, and L is the height of the receiver. Using these equations, the cosine coefficient can be calculated using Equation (23) [47].

$$\eta_{cos} = \frac{\sqrt{2}}{2} (\sin \alpha_s. \cos \lambda_s - \cos(\varphi_{surf} - \varphi_s). \cos \alpha_s. \sin \lambda_s + 1)^{0.5}$$
(23)

Finally, after calculating all the coefficients, the optical efficiency will be calculated.

3. Methodology

Given that the goal is to optimize the design of a heliostat field of a solar power plant with a central tower using the golden ratio of the Fibonacci sequence and to investigate the effect of this ratio on the field design results, it is necessary to introduce this sequence and the golden ratio in the first step.

3.1 Fibonacci sequence

An eminent Italian mathematician, Leonardo Pisano, first presented the concept of the Fibonacci sequence and its associated numbers. He is widely recognized by his nickname "Fibonacci," which has become synonymous with his work. The Fibonacci sequence is formed by summing the two preceding numbers in the series. The Fibonacci numbers are defined by Equation (24).

$$f_n = f_{n-1} + f_{n-2} (24)$$

For all n>=3, where f_n represents the nth Fibonacci Number. In geometry (Figure 4), a golden spiral is a logarithmic spiral whose growth factor is φ , the golden ratio. That is, a golden spiral gets wider (or further from its origin) by a factor of φ for every quarter turn it makes.

Fibonacci numbers spiral

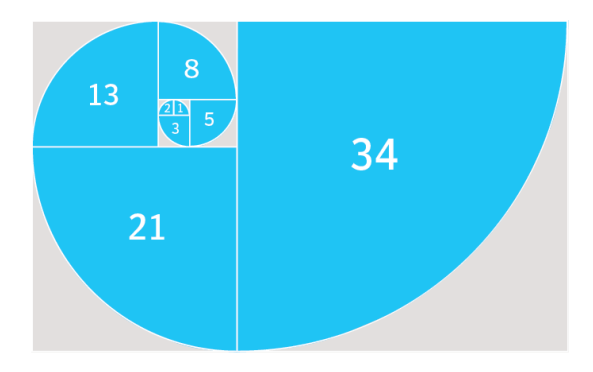


Figure 4. Fibonacci spiral geometry

The golden ratio, also referred to as the golden number, golden proportion, or the divine proportion, is a numerical ratio of around 1.618 between two numbers. Often represented by the Greek symbol phi, it is closely linked to the Fibonacci sequence, a numerical pattern where each number is the sum of the two preceding numbers.

The Golden Ratio is represented by the value 1.6184. This number has a connection to most things in our surroundings. These numbers alone are enough to unravel the major puzzle of the natural world. The ratio between two consecutive Fibonacci numbers is roughly equal to 1.6184. The remarkable aspect of this value is that when we multiply 0.618 by a Fibonacci number, the result is also a Fibonacci number. For example, when we multiply 5 by 0.618, we get approximately 3, which is also a Fibonacci number. Similarly, when we multiply 8 by 0.618, the result is approximately 5 is once again the number in the Fibonacci sequence.

In the next step, it is necessary to consider a study sample as a reference to study the effect of applying the golden ratio. The reference pattern used in this article is the radial staircase pattern. With the help of the relationships mentioned, the heliostat field can be designed in two cases. The first case is a field with normal design conditions, and the second case is one that considers the Fibonacci golden ratio in the distances between the mirrors. By performing calculations and comparing the results, it is possible to investigate the effect of this ratio on the design of the heliostat field. The field under study is located at latitude 19.7633 and longitude 96.0785, in Naypyidaw (the Capital of Myanmar). Other characteristics of the field under study are presented in Table 1.

Table 1. Reference heliostat field specifications

Variable	Value	Unit
Latitude	19.7633	-
Longitude	96.0785	-
Tower Height	95	m
Heliostat Height	7	m
Heliostat Length Size	11	m
Heliostat width Size	11	m
Number of Heliostat	1150	-
Separation Distance	0.2	m
Absorbing Aperture Height	20	m
Diameter of Reflected Spot	10	m
Reflector Length	8	m

First, using the existing equations, the field design values are calculated, and then, by affecting the value of the golden ratio, these values will be compared with the previous state. The design process is shown in Figure 5. According to Figure 5, initially, with the help of the equations in the design of the heliostat field, a design is made for a specific field, and with the help of modeling, the design values, including solar angles, field distances, number of rows, and optical coefficients, are calculated. In field design, attention is paid to the absence of collision of mirrors with each other, the absence of shading, and also the arrangement of the heliostat, which creates design limitations. In the second step, by affecting the golden ratio number in the distance between two consecutive rows and also in the radius of different zones around the central tower, once again the calculations related to the number of heliostats, the number of rows, the number of heliostats in each row and optical coefficients is done by completing the calculations in both cases, the results of the two models can be compared. At the end, the graphic design of the two fields is drawn, and any design flaws are checked in the final map. Finally, the evaluation of the solar thermal power received at the central tower is obtained using optical efficiency, which is calculated from the mirror reflection coefficient, the atmospheric attenuation coefficient, the shading and obstruction coefficient, and the cosine coefficient.

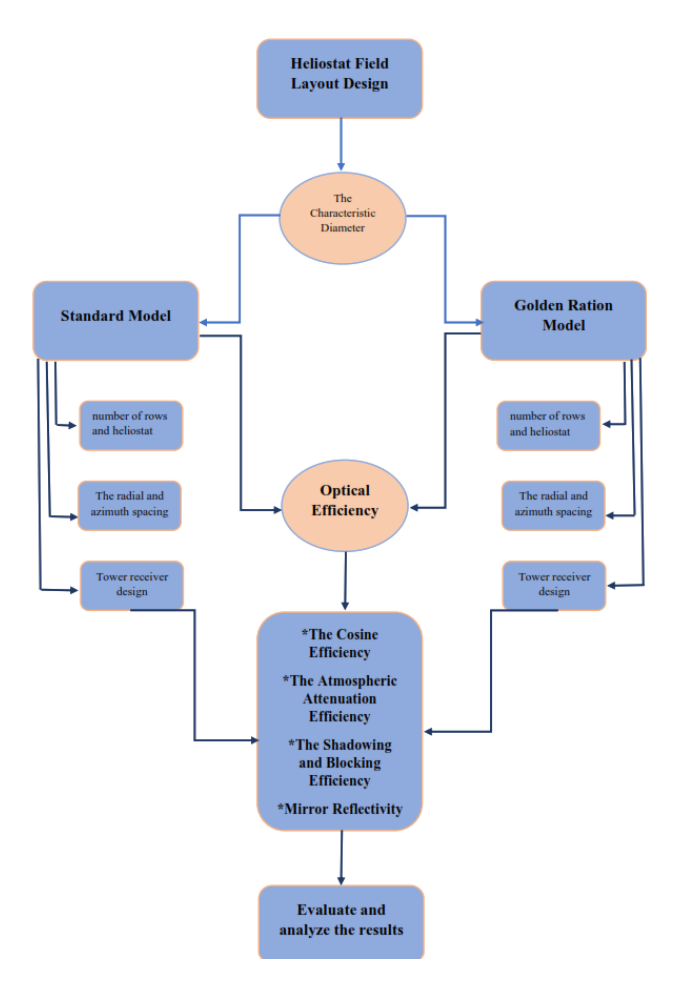


Figure 5. Heliostat field design flowchart

4. Results and discussion

Given that this study was conducted with the aim of evaluating the effect of using the golden number of the Fibonacci sequence on the performance of the heliostat field, it is necessary to first calculate the base field based on the specifications in Table 1. In the next step, assuming a constant number of heliostats, the changes caused by the golden ratio are considered to obtain the heliostat placement in the new arrangement. An important point in this regard is that the decision-making parameter in this study was the area required for the arrangement of mirrors and the optical efficiency of the field. In this regard, the field characteristics were first calculated through modeling in MATLAB, and then, based on that, the placement of the heliostats in the field will be drawn in two cases.

4.1 Results of heliostat field design

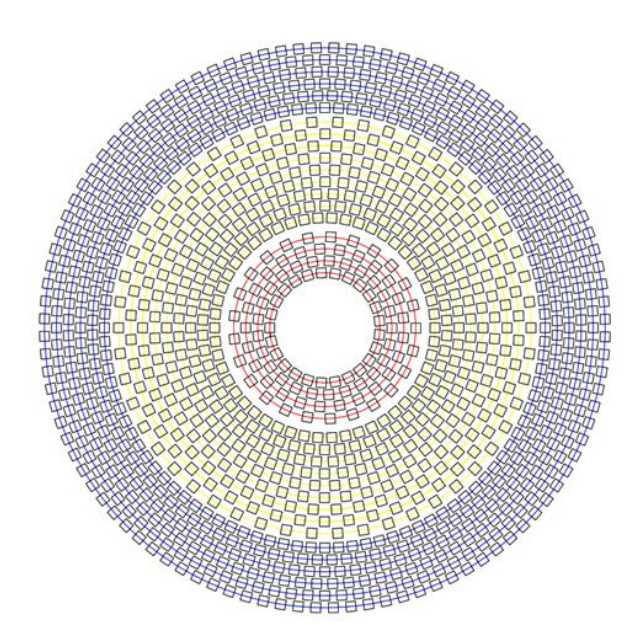
To design the field based on the specifications in Table 1, in the first step, the effective diameter and radial distance are calculated in each of the two scenarios: the base scenario and the scenario using the golden ratio. In the next step, the radius of the zones to the central tower, the azimuth angle, and the number of rows in each zone are obtained. Finally, by examining the variables related to the position of the sun and the performance coefficients, the light efficiency will be obtained.

Table 2. Detail design of two heliostat fields

It should be noted that to ensure the same design conditions, the position of the sun in both fields was based on the conditions of July 6 at 12 noon. Details of the designed fields are presented in Table 2.

To determine the number of rows in the third zone, as indicated in Table 1, one must subtract the total count of heliostats from the combined totals of the first and second zones. This calculation yields the number of heliostats present in the third zone. Subsequently, the number of heliostats per row in the third zone is calculated. Finally, by taking into account both the total number of heliostats in the third zone and the number of heliostats allocated to each row, the total number of rows in the third zone can be established. Also, Scenario calculations using the golden ratio have been made by applying the golden ratio $((1+\sqrt{5})/2)$ to the distances between the rows and designing the field assuming a constant number of heliostats. The designed fields and the placement of heliostats in each field are presented in Figure 6. According to Table 2 and Figure 6, and by comparing the two designed heliostat fields, it can be concluded that by affecting the golden ratio in the distances between the field rows, the total area of the solar power plant has increased by nearly 27%. Hence, the cost of land required for the power plant will increase.

Variable	Symbol	Base Scenario	Golden Ratio Scenario	Unit
Effective Diameter	DM	$11\sqrt{2}$	$11\sqrt{2} m$	m
Radial distance	ΔR_{min}	5.5√ 6	8.899√6	m
Radius of different zones to the central tower	R_1	$\frac{194.45}{\pi}$	100.1467	
	R_2	$\frac{388.90}{\pi}$	200.2933	m
	R_3	$\frac{777.8}{\pi}$	400.5867	
Azimuth angle for different zones	$\Delta a z_1$	0.2519	0.1555	
	Δaz_2	0.1257	0.0776	rad
	Δaz_3	0.0628	0.0388	
Number of circular pattern rows in each zone	$Nrow_1$	4	4	-
	$Nrow_2$	9	9	
	$Nrow_3$	6	2	
	$Nhel_1$	25	40	-
Number of heliostats in each row	$Nhel_2$	50	80	
	$Nhel_3$	100	135	
Number of heliostats in each zone	N_{z1}	100	160	-
	N_{z2}	450	720	
	N_{z3}	600	270	
Atmospheric attenuation coefficient	η_{at}	0.92	0.91	-
Solar position	δ_s	22.698		0
	h_s	0		
Solar altitude angle	α_s	87.0653		0
Zenith angle	θ_z	2.9347		0
Solar azimuth angle	φ_s	180		0
Azimuth angle of the surface	φ_{surf}	90		0
Angle of the reflected rays with the receiver aperture	θ_R	28.3586		o
Angle between the reflected rays and the line perpendicular to the receiver surface	λ_s	61.6414		0
Shading and blocking coefficient	$\eta_{s\&b}$	0.924	0.984	-
Cosine coefficient	η_{cos}	0.8586	0.8586	-
Optical efficiency	η_{opt}	0.7298	0.7688	-

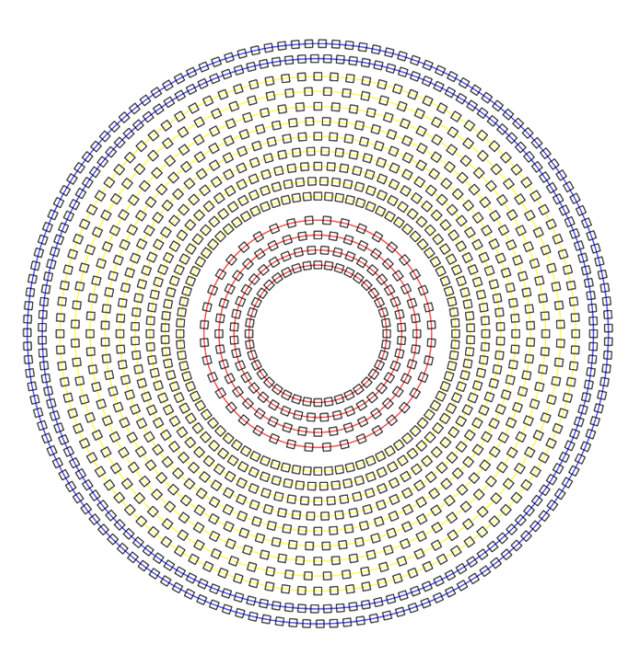


Base Scenario **Figure 6.** Configuration of designed fields

In the design, the number of heliostats was assumed to be constant for the purpose of comparing the optical efficiency coefficients, but considering the structure of the second field, this field can accommodate 130 more heliostats without increasing the current area of the field, which increases the number of heliostats by nearly 11% and the optical efficiency by 5.5% in this case, and the overall power of the power plant will also increase. The increase in optical efficiency in this case, considering the constant cosine coefficient in the two fields and the reduction of the atmospheric attenuation coefficient to 0.91 in the second field, can be considered the result of increasing the longitudinal distance of the rows from each other and increasing the average shading coefficient compared to the first field.

5. Conclusion

Considering the importance of developing the use of renewable resources and increasing the efficiency of energy production in various renewable systems, in this research, with the aim of improving the optical efficiency of heliostat solar power plants, the concept of Fibonacci and the golden ratio has been used as an interesting idea. The Fibonacci sequence is one of the most repeated concepts in nature that has always had good results. The effect of the golden ratio in the design of the radial stepped field of the heliostat power plant has not been investigated so far, and the aim of this article is to do this and obtain an innovative model in the design of heliostat fields. In this research, an attempt has been made to examine the changes in the heliostat field by examining the results of the design of the pattern based on the golden ratio and comparing it with the basic pattern. Also, while examining the design results, the optical efficiency coefficients, field characteristics, and the advances and limitations of the new field have been explained. In conclusion, the key results of this research can be summarized as follows:



Golden Ratio Scenario

- Using the golden ratio in the layout of a heliostat power plant increases the optical efficiency by 5.5% due to the increase in shading and blocking coefficients.
- Using the golden ratio in the configuration of heliostats, while keeping the number of heliostats constant, increases the area required for their arrangement by 27%.
- It should be noted that by increasing the area resulting from using the golden ratio in the arrangement of heliostats, the number of heliostats can be increased by 11% without increasing the current area.
- Increasing the area when using the golden ratio reduces the atmospheric attenuation coefficient to 0.91, resulting in a decrease in optical efficiency.

Ethical issue

The authors are aware of and comply with best practices in publication ethics, specifically concerning authorship (avoidance of guest authorship), dual submission, manipulation of figures, competing interests, and compliance with policies on research ethics. The authors adhere to publication requirements that the submitted work is original and has not been published elsewhere in any language.

Data availability statement

The manuscript contains all the data. However, more data will be available upon request from the corresponding author.

Conflict of interest

The authors declare no potential conflict of interest.

References

- [1] Jisoo Shim, Doosam Song, Unveiling energy inefficiencies: A study on building energy consumption in single-person households, Renewable and Sustainable Energy Reviews, Volume 214, 2025, doi: https://doi.org/10.1016/j.rser.2025.115546.
- [2] S. F. Moosavian, A. Hajinezhad, R. Fattahi, and A. Shahee, "Evaluating the effect of using nanofluids on the parabolic trough collector's performance," Energy

- Science & Engineering, vol. 11, no. 10, pp. 3512–3535, 2023.
- [3] Guixian Tian, Irfan Khan, Impact of energy end-uses and efficiency indicators on the environmental policy stringency index, Energy, Volume 326, 2025, 136232, doi: ttps://doi.org/10.1016/j.energy.2025.136232.
- [4] K. R. Abbasi, M. Shahbaz, J. Zhang, M. Irfan, and R. Alvarado, "Analyze the environmental sustainability factors of China: The role of fossil fuel energy and renewable energy," Renewable Energy, vol. 187, pp. 390–402, 2022.
- [5] H. H. Pourasl, R. V. Barenji, and V. M. Khojastehnezhad, "Solar energy status in the world: A comprehensive review," Energy Reports, vol. 10, pp. 3474–3493, 2023.
- [6] S. F. Moosavian, N. Mirzaei, A. Hajinezhad, H. Yousefi, R. Fattahi, and M. R. Golshadi, "Thermodynamic, Economic, and Environmental Evaluation of Municipal Waste Incinerator to Produce Power and Fresh Water," Energy Science & Engineering, 2025. doi: https://doi.org/10.1002/ese3.70263
- [7] T. Falope, L. Lao, D. Hanak, and D. Huo, "Hybrid energy system integration and management for solar energy: A review," Energy Conversion and Management: X, p. 100527, 2024.
- [8] M. Arun, Susmita Samal, Debabrata Barik, Sreejesh S.R. Chandran, Kapura Tudu, Seepana Praveenkumar, Integration of energy storage systems and grid modernization for reliable urban power management toward future energy sustainability, Journal of Energy Storage, Volume 114, Part B, 2025, https://doi.org/10.1016/j.est.2025.115830.
- [9] A. Kumler et al., "Potential effects of climate change and solar radiation modification on renewable energy resources," Renewable and Sustainable Energy Reviews, vol. 207, p. 114934, 2025.
- [10] R. M. Elavarasan, M. Nadarajah, and G. Shafiullah, "Multi-criteria decision analysis of clean energy technologies for envisioning sustainable development goal 7 in Australia: Is solar energy a game-changer?," Energy conversion and management, vol. 321, p. 119007, 2024.
- [11] M. Cellura, L. Q. Luu, F. Guarino, and S. Longo, "A review on life cycle environmental impacts of emerging solar cells," Science of The Total Environment, vol. 908, p. 168019, 2024.
- [12] Ugur Korkut Pata, Umit Bulut, Daniel Balsalobre-Lorente, Jana Chovancová, Does income growth affect renewable energy or carbon emissions first? A Fourier-based analysis for renewable and fossil energies, Energy Strategy Reviews, Volume 57, 2025, https://doi.org/10.1016/j.esr.2024.101615.
- [13] D. C. Nath et al., "Internet of Things integrated with solar energy applications: a state-of-the-art review," Environment, Development and Sustainability, vol. 26, no. 10, pp. 24597–24652, 2024.
- [14] G. Li, M. Li, R. Taylor, Y. Hao, G. Besagni, and C. Markides, "Solar energy utilisation: Current status and roll-out potential," Applied Thermal Engineering, vol. 209, p. 118285, 2022.

- [15] José L. Torres-Madroñero, Julian D. Osorio, César Nieto-Londoño, Juan C. Ordonez, Impact of molten salt inflow on the temperature distribution in thermal energy storage tanks at startup for central receiver concentrating solar power plants, Journal of Energy Storage, Volume 117, 2025, https://doi.org/10.1016/j.est.2025.116069.
- [16] A. N. Yerudkar, D. Kumar, V. H. Dalvi, S. V. Panse, V. R. Gaval, and J. B. Joshi, "Economically feasible solutions in concentrating solar power technology specifically for heliostats—A review," Renewable and Sustainable Energy Reviews, vol. 189, p. 113825, 2024.
- [17] L. A. Omeiza et al., "Application of solar thermal collectors for energy consumption in public buildings-An updated technical review," Journal of Engineering Research, 2023.
- [18] S. Wang et al., "Co-optimisation of the heliostat field and receiver for concentrated solar power plants," Applied Energy, vol. 348, p. 121513, 2023.
- [19] C. J. Noone, M. Torrilhon, and A. Mitsos, "Heliostat field optimization: A new computationally efficient model and biomimetic layout," Solar Energy, vol. 86, no. 2, pp. 792–803, 2012/02/01/ 2012, doi: https://doi.org/10.1016/j.solener.2011.12.007.
- [20] S. M. Besarati and D. Yogi Goswami, "A computationally efficient method for the design of the heliostat field for solar power tower plant," Renewable Energy, vol. 69, pp. 226–232, 2014/09/01/2014, doi: https://doi.org/10.1016/j.renene.2014.03.043.
- [21] A. Mutuberria, J. Pascual, M. Guisado, and F. Mallor,
 "Comparison of heliostat field layout design
 methodologies and impact on power plant efficiency,"
 Energy Procedia, vol. 69, pp. 1360–1370, 2015.
- [22] P. Richter, D. Laukamp, L. Gerdes, M. Frank, and a. E. Abrah'am, "Heliostat Field Layout Optimization with Evolutionary Algorithms," Artificial Intelligence, p. 13, 2016. https://doi.org/10.29007/7p6t
- [23] Deng et al., "Rose pattern for heliostat field optimization with a dynamic speciation-based mutation differential evolution," Int. J. Energy Res, 2020. https://doi.org/10.1002/er.5048
- [24] Q. Xie, Z. Guo, D. Liu, Z. Chen, Z. Shen, and X. Wang,
 "Optimization of heliostat field distribution based on
 improved Gray Wolf optimization algorithm,"
 Renewable Energy, vol. 176, pp. 447–458,
 2021/10/01/ 2021, doi:
 https://doi.org/10.1016/j.renene.2021.05.058.
- [25] E. Ghirardi, G. Brumana, G. Franchini, and A. Perdichizzi, "Heliostat layout optimization for loadfollowing solar tower plants," Renewable Energy, vol. 168, pp. 393–405, 2021/05/01/ 2021, doi: https://doi.org/10.1016/j.renene.2020.12.066.
- [26] K. Ali and S. Jifeng, "Research on modeling simulation and optimal layout of heliostat field optical efficiency for Solar Power Tower Plant," Applied Solar Energy, vol. 59, no. 6, pp. 957–977, 2023.
- [27] S. Babatunde and O. Abiola, "The Golden Ratio and Fibonacci Sequence in Nature."

 https://www.researchgate.net/profile/Abiola-Oyetoro/publication/378125611_The_Golden_Ratio_

- and_Fibonacci_Sequence_in_Nature/links/65c7cd6e3 4bbff5ba7fb8143/The-Golden-Ratio-and-Fibonacci-Sequence-in-Nature.pdf
- [28] Benguar, Alliah Nicole D., et al. "Golden ratio applied in the orientation of solar cells in a golden spiral solar panel." International Journal of Development Research 8.05 (2018): 20416-20420.
- [29] T. Nishiwaki and T. Yachi, "Arrangement of Fibonacci number photovoltaic modules for power generation woods," in 2014 International Conference on Renewable Energy Research and Application (ICRERA), 2014: IEEE, pp. 142–146.
- [30] H. Habibi, M. Zoghi, A. Chitsaz, K. Javaherdeh, M. Ayazpour, and E. Bellos, "Working fluid selection for regenerative supercritical Brayton cycle combined with bottoming ORC driven by molten salt solar power tower using energy–exergy analysis," Sustainable Energy Technologies and Assessments, vol. 39, p. 100699, 2020/06/01/2020, doi: https://doi.org/10.1016/j.seta.2020.100699.
- [31] B. Panbechi, A. Hajinezhad, S. F. Moosavian, and R. Fattahi, "Enhancing the enviro-economic viability of biogas-solar hybrid systems: Strategies for sustainable energy development in Iran," Energy Strategy Reviews, vol. 58, p. 101671, 2025/03/01/2025, doi: https://doi.org/10.1016/j.esr.2025.101671.
- [32] Hamid Hawi Ogaili, Shahram Khalilarya, Ata Chitsaz, Parisa Mojaver, Energy, exergy, and economic performance analysis of integrated parabolic trough collector with organic rankine cycle and ejector refrigeration cycle, Energy Conversion and Management: X, Volume 25, 2025, https://doi.org/10.1016/j.ecmx.2024.100843.
- [33] A. Herez, H. El Hage, T. Lemenand, M. Ramadan, and M. Khaled, "Review on photovoltaic/thermal hybrid solar collectors: Classifications, applications and new systems," Solar Energy, vol. 207, pp. 1321–1347, 2020.
- [34] Andi S. Ekariansyah, Martin Muwonge, M. Rifqi Saefuttamam, Yophie Dikaimana, Nasruddin, Energy, exergy, and exergy-economic optimization of a multigeneration system driven by geothermal primary heat source using multi-objective genetic algorithm (MOGA), Energy, Volume 330, 2025, https://doi.org/10.1016/j.energy.2025.136653.
- [35] J. B. Blackmon, "Heliostat size optimization for central receiver solar power plants," in Concentrating solar power technology: Elsevier, 2021, pp. 585–631.
- [36] J. Carballo et al., "Reinforcement learning for heliostat aiming: Improving the performance of Solar Tower plants," Applied Energy, vol. 377, p. 124574, 2025.
- [37] M. Maiga, K. E. N'Tsoukpoe, A. Gomna, and Y. K. Fiagbe, "Sources of solar tracking errors and correction strategies for heliostats," Renewable and Sustainable Energy Reviews, vol. 203, p. 114770, 2024.

- [38] C. B. Anderson, G. Picotti, M. E. Cholette, B. Leslie, T. A. Steinberg, and G. Manzolini, "Heliostat-field soiling predictions and cleaning resource optimization for solar tower plants," Applied Energy, vol. 352, p. 121963, 2023.
- [39] J. Baigorri, F. Zaversky, and D. Astrain, "Massive gridscale energy storage for next-generation concentrated solar power: A review of the potential emerging concepts," Renewable and Sustainable Energy Reviews, vol. 185, p. 113633, 2023.
- [40] A. H. Alami et al., "Concentrating solar power (CSP) technologies: Status and analysis," International Journal of Thermofluids, vol. 18, p. 100340, 2023.
- [41] F. J. Collado and J. Guallar, "Campo: Generation of regular heliostat fields," Renewable energy, vol. 46, pp. 49–59, 2012.
- [42] M. Saghafifar, "Thermo-economic optimization of hybrid combined power cycles using heliostat field collector," 2016. http://hdl.handle.net/11073/8103.
- [43] M. Atif and F. A. Al-Sulaiman, "Development of a mathematical model for optimizing a heliostat field layout using differential evolution method," International Journal of Energy Research, vol. 39, no. 9, pp. 1241–1255, 2015.
- [44] C. Shen, Y.-L. He, Y.-W. Liu, and W.-Q. Tao, "Modelling and simulation of solar radiation data processing with Simulink," Simulation Modelling Practice and Theory, vol. 16, no. 7, pp. 721–735, 2008.
- [45] K. Jazayeri, S. Uysal, and M. Jazayeri, "MATLAB/simulink based simulation of solar incidence angle and the sun's position in the sky with respect to observation points on the Earth," in 2013 International Conference on Renewable Energy Research and Applications (ICRERA), 2013: IEEE, pp. 173–177.
- [46] Y. Yao, Y. Hu, and S. Gao, "Heliostat field layout methodology in central receiver systems based on efficiency-related distribution," Solar energy, vol. 117, pp. 114–124, 2015.
- [47] X. Wei, Z. Lu, Z. Wang, W. Yu, H. Zhang, and Z. Yao, "A new method for the design of the heliostat field layout for solar tower power plant," Renewable Energy, vol. 35, no. 9, pp. 1970–1975, 2010/09/01/2010, doi: https://doi.org/10.1016/j.renene.2010.01.026.



This article is an open-access article distributed under the terms and conditions of the Creative Commons Attribution (CC BY) license

(https://creativecommons.org/licenses/by/4.0/).